Second harmonic generation in GF(*m*, 1) ferroelectric superlattices

2006 J. Phys.: Condens. Matter 18 2587

(http://iopscience.iop.org/0953-8984/18/8/020)

INSTITUTE OF PHYSICS PUBLISHING JOURNAL OF PHYSICS: CONDENSED MATTER

J. Phys.: Condens. Matter **18** (2006) 2587–2600 doi:10.1088/0953-8984/18/8/020

Second harmonic generation in GF(m, 1) ferroelectric superlattices

Ying Chen[1], **Xiangbo Yang**[1,3], **Qi Guo**[2] **and Sheng Lan**[2]

[1] Institute of Laser Life Science, South China Normal University, Guangzhou 510631, People's Republic of China
[2] Laboratory of Photonic Information Technology, South China Normal University, Guangzhou 510631, People's Republic of China

E-mail: xbyang@scnu.edu.cn

Received 26 September 2005, in final form 3 January 2006
Published 10 February 2006
Online at stacks.iop.org/JPhysCM/18/2587

Abstract

In this paper we study under the small-signal approximation the properties of the output electric field of second harmonic generation (SHG) for vertical transmission in Family A of the generalized Fibonacci (GF(m, 1)) quasiperiodic ferroelectric domain system. It is found that under perfect quasi-phase-matched (PQPM) conditions there exists self-similarity for the intense peaks of SHG (IPSHG) in real space and the two integers q and p indexing IPSHG make an interesting zero–odd set when m is large enough. On the other hand, self-similarity for IPSHG is broken under imperfect quasi-phase-matched (IQPM) conditions and the SHG spectra comprise a group of intense peaks and another group of satellite weak lines when m is very large. The corresponding integers q and p make an interesting odd–odd set and a successive integer set, respectively. Two kinds of effects of vacancies on SHG have also been found. The analytical results are confirmed by numerical simulations.

1. Introduction

Since the important discovery by Shechtman *et al* [1] of a diffraction pattern with fivefold symmetry, much attention has been given to the investigation of the optical properties of quasilattices and multilayer systems arranged following quasiperiodic sequences. The Fibonacci model (FC(1)) is the most studied quasiperiodic sequence because its structure not only possesses the main characteristics of quasicrystals but is also relatively simple. Using molecular-beam epitaxy, Merlin *et al* [2] in 1985 fabricated the first quasiperiodic semiconductor superlattice, consisting of alternating layers of GaAs and AlAs to form an FC(1) sequence. Tamura and Wolfe [3] made a theoretical study of acoustic-phonon transmission through a realistic FC(1) superlattice and obtained some results for the transmission spectra. Zhu and Ming [4] investigated theoretically the second harmonic generation (SHG) in an

[3] Author to whom any correspondence should be addressed.

FC(1) optical superlattice made from a single crystal with a quasiperiodic laminar ferroelectric domain structure. Zhu *et al* [5] fabricated a nonlinear optical superlattice of $LiTaO_3$ in which two building blocks, A and B, were arranged as an FC(1) sequence and measured its SHG spectra. They also researched the characteristics of SHG through the Thue–Mouse system [6], the intergrowth system [7] and the three-component Fibonacci system [8, 9], respectively. Yang and Liu [10, 11] studied the properties of SHG through Fibonacci-class (FC(n)) ferroelectric domains, which are perfect extensions of FC(1), found an interesting self-similarity of the brightest peaks and obtained the output power per unit area of SHG.

Generalized Fibonacci models (GF(m, n)) are another kind of general extension of FC(1) and were firstly systematically investigated by Gumbs and Ali [12] in 1988. They can be generated by the substitution rules

$$B \to A, \qquad A \to A^m B^n, \tag{1}$$

where m and n are all positive integers. Generally, GF(m, 1) is defined as Family A of GF(m, n) while GF(1, n) is defined as Family B of GF(m, n), and their associated substitution matrices are as follows:

$$M_A = \begin{pmatrix} m & 1 \\ 1 & 0 \end{pmatrix} \tag{2}$$

and

$$M_B = \begin{pmatrix} 1 & n \\ 1 & 0 \end{pmatrix}. \tag{3}$$

The corresponding eigenvalues of M_A and M_B are

$$\tau_{A\pm} = \frac{m \pm \sqrt{m^2+4}}{2} \tag{4}$$

and

$$\tau_{B\pm} = \frac{2 \pm \sqrt{1+4n}}{2}, \tag{5}$$

respectively. This shows that M_A satisfies the Pisot condition and the unit determinant requirement [13]. Therefore, GF(m, 1) are real quasiperiodic models and have a volume-preserving trace map and a Cantor-like energy spectrum with critical electronic states [14]. Unfortunately, GF(1, n) are non-quasiperiodic models and have a volume-non-preserving trace map and a Bloch-like part as well as a singular part of the energy spectrum such that extended electronic states are allowed.

Interest in GF(m, n) has increased since it appears that in some fundamental aspects the physical properties of the Fibonaccian quasicrystal may not be genetic [15]. Costa Filho and Albuquerque [16] researched fractal aspects of the spin wave spectra in pure and generalized Fibonacci anisotropic magnetic superlattices. Mauriz *et al* [17] investigated the specific heat properties of electrons in one-dimensional (1D) GF(m, n) aperiodic potentials. Tyc and Salejda [18] formulated a quantum-mechanical model of electron ballistic transport in GF(m, n) semiconductor superlattices. As for the transmission properties of light, Kohmoto *et al* [19] considered light propagation through an optical Fibonaccian (GF(1, 1)) multilayer. Dulea *et al* [15] reported optical transmission through multilayers arranged according to families A and B of GF(m, n). Klauzer-Kruszyna *et al* [20, 21] developed a theory of polarized light propagation in dielectric GF(m, n) multilayers and also presented the numerical results of transmittance. Recently, Li and Yang [22] have studied the transmission properties of light normally through aperiodic GF(m, n) multilayers.

In this paper we investigate the properties of SHG through GF(m, 1) ferroelectric domains, as GF(1, n) are non-quasiperiodic sequences and cannot be obtained by the projection method.

It is found that, under the perfect quasi-phase-matched (PQPM) condition, and when m is large enough, the intense peaks of SHG (IPSHG) locate at odd times of the coherence length and the two integers indexing IPSHG make an interesting zero–odd set. Under imperfect quasi-phase-matched (IQPM) conditions, a new group of weak satellite lines occur and the corresponding integers make an interesting odd–odd set and a successive integers set. Additionally, we also propose a possible solution for the structure of imperfect quasiperiodic superlattices to fit the PQPM condition.

We organize our paper as follows: the projection method of GF(m, 1) is introduced in section 2, the characteristics of SHG under PQPM are investigated in section 3, section 4 is devoted to a discussion of the case under IQPM conditions. Self-similarity and the effect of vacancies are researched in section 5, and section 6 gives a brief summary.

2. The characteristic construction of GF(m, 1)

By means of substitution in equation (1) one can obtain GF(m, 1) as follows:

$$B \to A, \qquad A \to A^m B. \tag{6}$$

Starting with a A, the first three generations of GF(m, 1) are

$$\begin{aligned} G_1 &= A \\ G_2 &= A^m B \\ G_3 &= \underbrace{(A^m B)(A^m B)\cdots(A^m B)}_{m} A, \end{aligned} \tag{7}$$

which show the following recurring relation

$$G_h = G_{h-1}^m G_{h-2} \qquad (h \geqslant 3). \tag{8}$$

Additionally, one can also obtain GF(m, 1) sequences by a projection method from a two-dimensional (2D) square lattice. As an example, the GF(2, 1) sequence is illustrated in figure 1. From the coordinate origin, one can draw a projection line (PL) with projection angle θ, which satisfies [23]

$$\tan\theta = \frac{1}{\delta_m} = \frac{\sqrt{m^2+4}-(2-m)}{2m}, \tag{9}$$

where

$$\delta_m = 1 + \frac{1}{\tau_m} = \frac{\sqrt{m^2+4}+2-m}{2}, \tag{10}$$

and the eigenvalue

$$\tau_m = \tau_{A+} = \frac{m+\sqrt{m^2+4}}{2}. \tag{11}$$

At the same time, the eigenvalue τ_m also fits into the following limit value [14]

$$\tau_m = \lim_{h\to\infty} \frac{\mathrm{GF}(m,1)_h}{\mathrm{GF}(m,1)_{h-1}}, \tag{12}$$

where GF(m, 1)$_h$ is the number of elements for the hth generation of GF(m, 1).

We make the lower right-hand vertices (hollow circles) of the unit cells, which the PL has passed through, project to the PL only when the higher ones are not projecting points. Then one can obtain a set of points (solid circles) on the PL which have the following positions along the PL from the origin:

$$P_N = N\cos\theta + \sin\theta\lfloor N\tan\theta\rfloor, \tag{13}$$

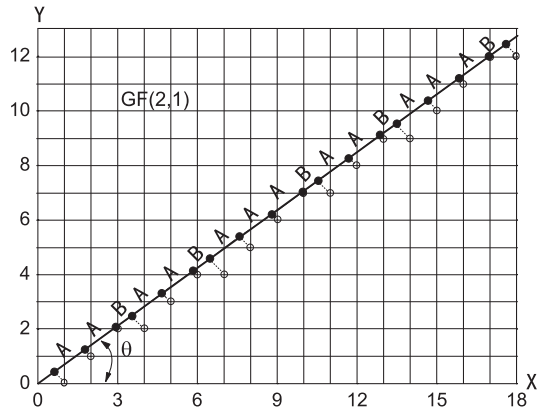

Figure 1. Illustration for obtaining the GF(2, 1) sequence with projection method, where $\tan\theta = \sqrt{2}/2$.

where $\lfloor\ \rfloor$'s represent the greatest integer function. We call the long segments on the PL A cells, the lengths of which are $\cos\theta + \sin\theta$, and the short ones B cells, the lengths of which are $\cos\theta$, then A and B cells construct GF(m, 1) sequences. In figure 1, for the GF(2, 1) sequence, $\tan\theta = \sqrt{2}/2$, $A = (\sqrt{3} + \sqrt{6})/3$, and $B = \sqrt{6}/3$.

3. The output electric field of SHG E_2 under PQPM conditions

3.1. The formula of E_2

The GF(m, 1) ferroelectric systems being studied in this paper are made up of $LiNbO_3$. First we construct two building blocks A and B containing one positive ferroelectric domain and one negative one, shown in figure 2(b). In order to explore the largest second-order nonlinear optical coefficient d_{33} of the material, one can make the interfaces of each domain parallel to the y–z plane and the polarization of the electric fields along the z-axis with the propagating directions along the x-axis. From figure 2(a) one can see that the coordinate x_N, which is the position of the Nth layer of the ferroelectric domain boundary, can be written as follows [23]:

$$x_N = Nl_B + (l_A - l_B)\left\lfloor \frac{N}{\delta_m} \right\rfloor, \tag{14}$$

where l_A (l_B) is the thickness of block A (B). Secondly, in order to make the superlattice system fit the PQPM condition, we try to set that

$$\begin{aligned} &l_A/l_B = \delta_m \\ &l_A^+ = l \\ &l_A^- = l(1+\eta) \\ &l_B^+ = l \\ &l_B^- = l(1-\tau_m\eta), \end{aligned} \tag{15}$$

where

$$\eta = \frac{2(\delta_m - 1)}{1 + \delta_m\tau_m} = \frac{(m+2)\sqrt{m^2+4} - m^2 - 2m - 2}{2m+3}, \tag{16}$$

and l is adjustable structure parameter.

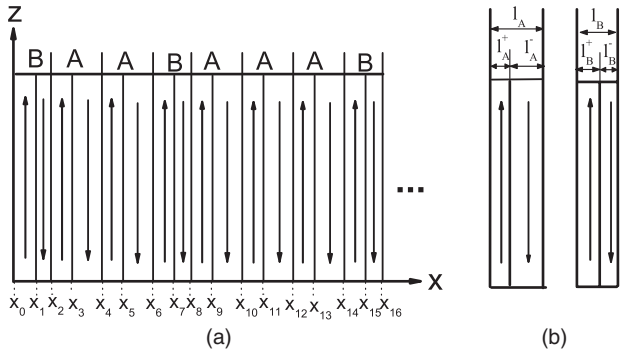

Figure 2. The ferroelectric multilayers constitute a GF(2, 1) sequence superlattice, where the directions of the arrows indicate the polarization orientation of the electric fields. (a) The schematic diagram of the total ferroelectric superlattice, where the coordinate $\{x_N\}$ is the position of the Nth layer domain boundary. (b) Two building blocks, A and B, each comprising one positive and one negative ferroelectric domain.

Under the small-signal approximation the electric field of the fundamental beam (FB) E_1 and that of SHG E_2 satisfy the following wave equations [4, 24]:

$$\begin{aligned} \frac{\mathrm{d}E_1(x)}{\mathrm{d}x} &= 0 \\ \frac{\mathrm{d}E_2(x)}{\mathrm{d}x} &= \frac{-\mathrm{i}32\pi\omega^2}{k_2c^2}d(x)E_1^2\mathrm{e}^{\mathrm{i}(k_2-2k_1)x}, \end{aligned} \tag{17}$$

where

$$d(x) = \begin{cases} d_{33}, & \text{in positive ferroelectric domains} \\ -d_{33}, & \text{in negative ferroelectric domains,} \end{cases} \tag{18}$$

ω is the angular frequency of the FB, k_1 and k_2 are the wavenumbers of the FB and the SHG, respectively, and c is the speed of light in a vacuum. After passing through N layers of GF(m, 1) ferroelectric domains the electric field E_2 can be presented as

$$E_2(N) = \frac{-64\pi\omega^2}{k_2c^2\Delta k}d_{33}E_1^2\left(\sum_{j=0}\mathrm{e}^{\mathrm{i}\Delta k x_{2j+1}} - \sum_{j=0}\mathrm{e}^{\mathrm{i}\Delta k x_{2j}}\right), \tag{19}$$

where

$$\Delta\mathbf{k} = \mathbf{k}_2 - 2\mathbf{k}_1, \tag{20}$$

and the relationship between the wavenumber and the refractive indices satisfies [25]

$$\Delta k = |\Delta\mathbf{k}| = \frac{4\pi}{\lambda}(n_2 - n_1), \tag{21}$$

where n_2 and n_1 are the refractive indices of SHG and FB, respectively.

GF(m, 1) are quasiperiodic sequences, and the structure of the systems satisfies equations (14) and (15). Then one can see that in the reciprocal space the Fourier transform of the layer positions of GF(m, 1) superlattices will consist of Bragg peaks [26, 27] at positions

$$k_{pq} = \frac{2\pi}{D}(p\delta_m + q), \tag{22}$$

where p and q are integers, and

$$D = l_B\delta_m + l_A - l_B. \tag{23}$$

Then the output electric field of SHG E_2 of GF(m, 1) superlattices can be represented as follows:

$$E_2(N) \approx -\frac{128\pi\omega^2}{k_2c^2\Delta k}(d_{33}E_1^2)\mathrm{e}^{\frac{\mathrm{i}}{2}(\pi+\Delta kl)}\sin\left(\frac{\Delta kl}{2}\right)\sum_{pq}\mathrm{e}^{\mathrm{i}Y_{pq}}\left(\frac{\sin Y_{pq}}{Y_{pq}}\right)\delta(\Delta k - k_{pq}), \tag{24}$$

where

$$Y_{pq} = \frac{\pi\delta_m}{D}[ql_B - p(l_A - l_B)]. \tag{25}$$

3.2. The tendency of SHG spectra

Generally, the intensity of the electric field of SHG $I(2\omega)$ can be defined as follows:

$$I(2\omega) = |E_2|^2. \tag{26}$$

By means of equations (24) and (26), one can obtain the relative intensity of SHG. In order to compare our results with the corresponding numerical simulations [4, 10] and experimental data [5] for Fibonacci superlattices, we choose $\lambda_0 = 1.318$ μm and the structure parameter l changes from 0.0 to 65.0 μm in real space. For the special wavelength of FB λ_0, the refractive indices n_2 and n_1 are all constant. For $LiNbO_3$, $n_{10} = 2.1453$ and $n_{20} = 2.1970$ [28].

Figures 3(a)–(c) show the cases of GF(1, 1), GF(4, 1) and GF(8, 1) in real space. One can see that when m is relatively very small there are not only some intense peaks but also an abundance of weak peaks appearing in the SHG spectra, and the spectral structure is very complicated. The reason for this is that, in comparison with periodic models, GF(m, 1) are normal quasiperiodic sequences and have a lower space-group symmetry and more Fourier distributions. This would provide more reciprocal-lattice vectors to compensate for the mismatching phase among interacting waves and would make the SHG spectral structure more complex.

From figures 3(d)–(f) one can see that with increasing m the weak peaks will disappear completely and the spectral lines tend to be composed of only a set of intense peaks with equivalent intensity and the positions locate at the odd times of the coherence length of SHG l_c, which can be defined as follows: [29]

$$l_c = \frac{\lambda_0}{4(n_{20} - n_{10})}. \tag{27}$$

For $LiNbO_3$ material, if the aforementioned data are chosen then one can obtain the coherence length l_c as follows:

$$l_c = 6.3733\ \mu\mathrm{m}. \tag{28}$$

Finally, when m is big enough, the two integers q and p indexing the IPSHG would make an interesting zero–odd set as follows:

$$\lim_{m\to\infty}\{q, p\}_{\mathrm{intense}} = \{0, 2j+1\}, \qquad (j \geqslant 0). \tag{29}$$

This can be explained as follows.

With the increase in m, the proportion of B blocks becomes smaller and smaller and the real quasiperiodic sequences would change to approximately periodic ones. On the other hand, by means of equations (10), (11) and (14)–(16), one can also obtain that

$$\begin{aligned}
&\lim_{m\to\infty}\delta_m = 1\\
&\lim_{m\to\infty}\tau_m = \infty\\
&\lim_{m\to\infty}\eta = 0\\
&\lim_{m\to\infty}l_A^+ = l_A^- = l_B^+ = l_B^- = l\\
&\lim_{m\to\infty}x_N = Nl_A.
\end{aligned} \tag{30}$$

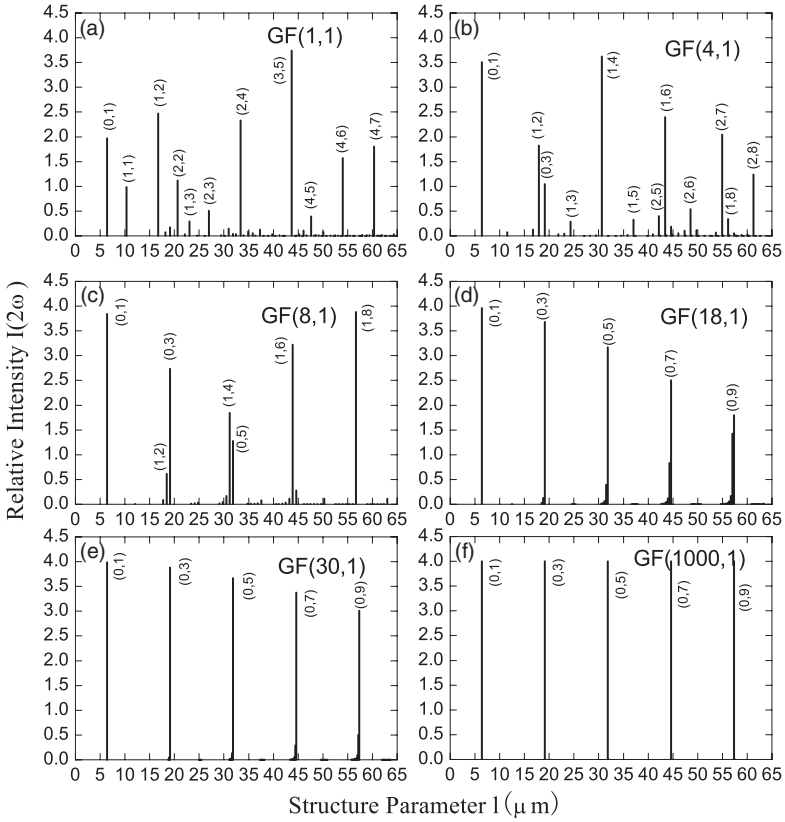

Figure 3. In real space, the figure of SHG relative intensity $I(2\omega)$ versus structure parameter l under PQPM conditions, where for $LiNbO_3$ $\lambda_0 = 1.318$ μm, $n_{10} = 2.1453$, and $n_{20} = 2.1970$.

Obviously, this is a simple periodic structure. On the other hand, the same conclusion can be deduced from the projection method. If m is large enough, then the projection angle θ tends to $\pi/4$ (see equation (9)), i.e. the PL tends to the diagonal of 2D square lattices (shown in figure 1). Of course, the lengths of the cells A and B on the PL would tend to be equivalent and they construct a periodic sequence. In a word, this kind of 1D GF(m, 1) sequence is quite different from some 2D quasicrystals (e.g. the 2D Penrose tiling, the 2D dodecagonal quasicrystal, etc). While the scales of the latter tend to be infinite, their characteristics are still quasiperiodic, for their symmetries are mainly dependent on their central structures. However, the former posses interesting asymptotic properties and would tend to be like periodic structures when the parameter m is large enough. Then it is possible for us to deal with the tendency of SHG spectra in the same way as for the spectra of periodic sequences.

From [30] it is known that IPSHG can occur only when the reciprocal-lattice vectors of a periodic system G_n satisfy the following relation

$$\Delta k - G_n = \frac{4\pi}{\lambda_0}(n_{20} - n_{10}) - \frac{2\pi n}{\Lambda} = 0, \tag{31}$$

where n is a positive integer and $\Lambda = 2l$ is the period of the superlattice. Equation (31) can be also rewritten as follows:

$$\frac{\pi}{l_c} - \frac{2\pi n}{2l} = 0 \Rightarrow l = nl_c. \tag{32}$$

On the other hand, the effect of vacancies would be to modulate IPSHG by the parameter $\sin(\Delta kl/2)$ (see equation (24)). Consequently, for periodic multilayers systems, the structure parameter l for IPSHG should be equal to odd times of l_c (i.e. the positions can be labelled by only one odd number) and the SHG spectra would comprise purely intense peaks.

Additionally, by means of equations (21)–(23), we find that in real space the structure parameter l of SHG peaks for GF(m, 1) quasiperiodic superlattices can be presented as follows:

$$l_{qp} = l_c\left(\frac{q}{\delta_m} + p\right). \tag{33}$$

When m is large enough, GF(m, 1) tend to be periodic sequences and only the peaks indexed by one odd number could maintain a relatively high intensity, then the integers q and p should be equal to zero and an odd number, respectively. This is the reason why integers q and p comprise the zero–odd set in equation (29).

In figure 3 (f), $m = 1000$ and

$$\begin{aligned} l_{(0,1)} &= 6.3733\ \mu\text{m} = l_c \\ l_{(0,3)} &= 19.1199\ \mu\text{m} = 3l_c \\ l_{(0,5)} &= 31.8665\ \mu\text{m} = 5l_c \\ l_{(0,7)} &= 44.6132\ \mu\text{m} = 7l_c \\ l_{(0,9)} &= 57.3598\ \mu\text{m} = 9l_c. \end{aligned} \tag{34}$$

Obviously, the analytical results are confirmed by the numerical simulations.

In the reciprocal space, the structure parameter l is kept constant and has been chosen to be l_c. Figure 4 shows the relation between the relative intensity of SHG peaks $I(2\omega)$ and the wavelength of FB λ. One can see that the properties in reciprocal space are similar to those in real space. When m is relatively very small, there are many SHG peaks, intense ones and weak ones, and the structure of the SHG spectra is very complicated (see figures 4(a) and (b)), but when m is not very small, the weak peaks disappear gradually and the spectral lines mainly consist of several intense peaks (see figures 4(c)–(e)). Consequently, when m is big enough, the weak peaks will disappear completely and only a set of intense peaks with equivalent intensity are left (see figure 4(f)). The principle is as the same as that in real space.

4. The output electric field of SHG E_2 under IQPM conditions

By means of equations (6)–(8), one can see that although GF(1, 1) and FC(1) are the same model and GF(m, 1) and FC(n) [31] are all extensions of FC(1), the symmetry of the former is quite different from that of the latter. Consequently, the PQPM condition for generating SHG of the former ferroelectric superlattice would be, of course, different from that of the latter. For the former, we choose the structure confined by equations (14)–(16), where two irrationals δ_m and τ_m are used, and obtain the interesting tendency of the spectra of SHG, which has been discussed in detail in section 3.2.

In order to explore the influence of PQPM conditions on the SHG spectra, we choose another set of structure conditions as follows:

$$x_N = N + \frac{1}{\delta_m}\left\lfloor\frac{N}{\delta_m}\right\rfloor, \tag{35}$$

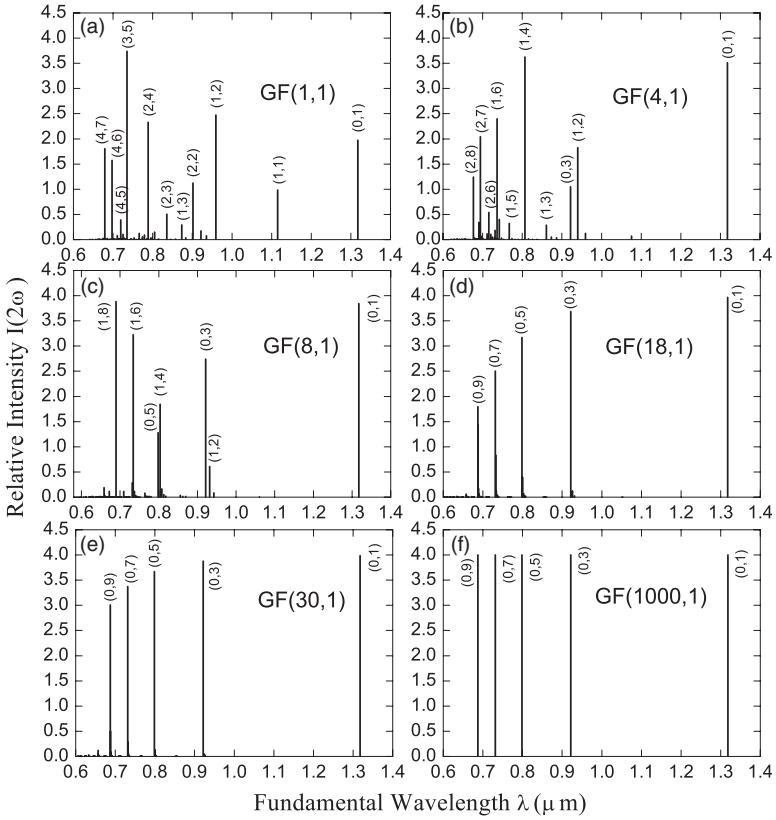

Figure 4. In reciprocal space, the figure of relative intensity of SHG $I(2\omega)$ versus fundamental wavelength λ under PQPM conditions, where for $LiNbO_3$ $l_c = 6.373$ μm.

$$
\begin{aligned}
&l_A/l_B = \delta_m \\
&l_A^+ = l \\
&l_A^- = l(1+\eta) \\
&l_B^+ = l \\
&l_B^- = l(1-\delta_m\eta),
\end{aligned}
\tag{36}
$$

and

$$
\eta = \frac{2(\delta_m - 1)}{1+\delta_m^2} = \frac{3\sqrt{m^2+4} - m - 4}{2m^2 - 2m + 5}, \tag{37}
$$

where only one irrational δ_m is used. This is similar to the conditions for FC(n) [10].

For this condition one can find that the structures for GF(m, 1) systems do not fit the PQPM condition but only satisfy the IQPM one. One can also deduce that the formula for E_2 of GF(m, 1) superlattices has the same form as that of equation (24), but the corresponding variables here are not the same; they can be written as follows:

$$
\begin{aligned}
&Y_{pq} = \frac{\pi\delta_m}{1+\delta_m^2}(q\delta_m - p) \\
&D = l_A\delta_m + l_B \\
&l_{qp} = l_c\frac{q + p\delta_m}{1+\delta_m}.
\end{aligned}
\tag{38}
$$

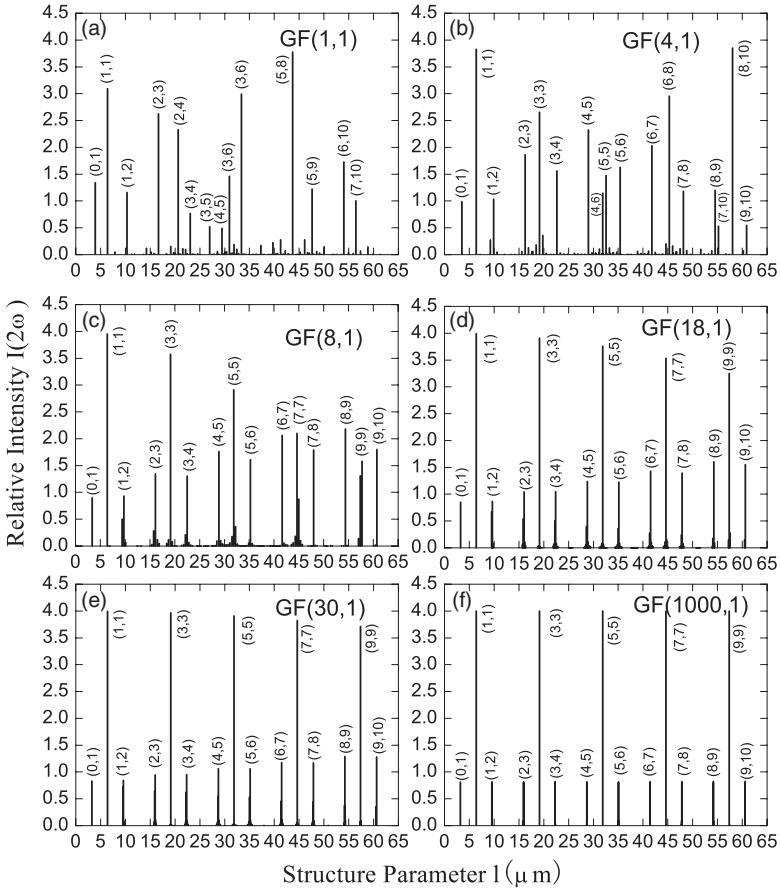

Figure 5. In real space, the figure of SHG spectra under IQPM conditions, where the corresponding parameters are as the same as those in figure 3.

We draw the figure of the SHG spectra in real space in figure 5 and find that when m is not very large there are also plentiful intense and weak peaks and the number of lines is about three times that under PQPM conditions. When m is large enough, the two integers q and p indexing IPSHG make a new interesting odd–odd set as follows:

$$\lim_{m\to\infty}\{q,\,p\}_{\text{intense}} = \{2j+1,\,2j+1\}, \qquad (j \geqslant 0). \tag{39}$$

At the same time, each intense peak is surrounded by two satellite peaks, where the two integers q and p construct the following even–odd and odd–even sets:

$$\lim_{m\to\infty}\{q,\,p\}_{\text{satellite}} = \begin{cases} \{2j,\,2j+1\} \\ \{2j+1,\,2j+2\}, \end{cases} \qquad (j \geqslant 0). \tag{40}$$

These new phenomena can be explained as follows. The structure defined in equations (35)–(37) only fits the IQPM condition, but not the PQPM condition as in section 3. The reason for this is that GF(m, 1) are not perfect quasiperiodic sequences and the substitution method for generating GF(m, 1) is not completely in accord with the corresponding projection method. From equations (9), (10) and (12), we find that the limit value τ_m of the substitution method is not directly a count-down of the tangent value δ_m of the projection angle. This means

that the structures of GF(m, 1)s fitting the PQPM condition should be dependent on both τ_m and δ_m. This is quite different from that of FC(n), which are a class of perfect quasiperiodic sequences [10]. This is the very reason that in section 3, in order to make the system fit PQPM conditions, we chose τ_m and δ_m to confine the structure jointly. In order to compare the symmetry of GF(m, 1) sequences with that of FC(n) ones, we list the PQPM structure conditions of the latter in [10] as follows:

$$\begin{aligned} &l_A/l_B = \varphi_n \\ &l_A^+ = l \\ &l_A^- = l(1+\eta) \\ &l_B^+ = l \\ &l_B^- = l(1-\varphi_n\eta), \end{aligned} \tag{41}$$

where

$$\eta = \frac{2(\varphi_n - 1)}{1+\varphi_n^2} = \frac{3\sqrt{n^2+4} - n - 6}{2n+3}. \tag{42}$$

From equation (41) one knows that for FC(n) sequences the substitution method is in accord with the projection one and the structures fitting PQPM conditions are dependent on only one parameter φ_n. The SHG spectra of FC(n) are shown in figure 6, and one can see that the properties of their spectral lines are similar to those of GF(m, 1) in section 3 (see figure 3) but are different from those of GF(m, 1) in section 4 (see figure 5). The same set as equation (29) can also be found when n is very large (see figure 6(f)).

In this section, one of the results for fitting IQPM is the generation of satellite peaks, because the space-group symmetry of the systems is lower than that in section 3 and has more reciprocal vector distributions. The other result for fitting IQPM is the changing of the positions of the SHG peaks l_{qp} (see equations (33) and (38)) and the variation of the relative intensity $I(2\omega)$.

5. The self-similarity of intense peaks and the effect of vacancies on SHG

5.1. The self-similarity of intense peaks

From equation (24) one can see that when $\Delta k = k_{pq}$ and $Y_{pq} \to 0$ the SHG lines are intense peaks. By means of equations (33) and (38), one can obtain the ratio of integers p and q indexing intense peaks for the following two cases:

$$\begin{aligned} &\text{PQPM}: \quad p/q \to \tau_m \\ &\text{IQPM}: \quad p/q \to \delta_m. \end{aligned} \tag{43}$$

By use of equation (12) one can obtain the property of the structure parameter l of IPSHG as follows:

$$\begin{aligned} &\text{PQPM}: \quad l_{qp} = l_{\mathrm{GF}(m,1)_{h-1},\mathrm{GF}(m,1)_h} = l_h \\ &\text{IQPM}: \quad l_{qp} \neq l_{\mathrm{GF}(m,1)_{h-1},\mathrm{GF}(m,1)_h} = l_h, \end{aligned} \qquad (h \geqslant 2). \tag{44}$$

Consequently,

$$\begin{aligned} &\text{PQPM}: \quad l_{h-1} + ml_h = l_{h+1} \\ &\text{IQPM}: \quad l_{h-1} + ml_h \neq l_{h+1}, \end{aligned} \qquad (h \geqslant 2). \tag{45}$$

In real space, the wavelength of FB λ_0 is kept constant and the effect of the dispersion of refractive indices on SHG has not been taken into account. From equation (44) one can see that

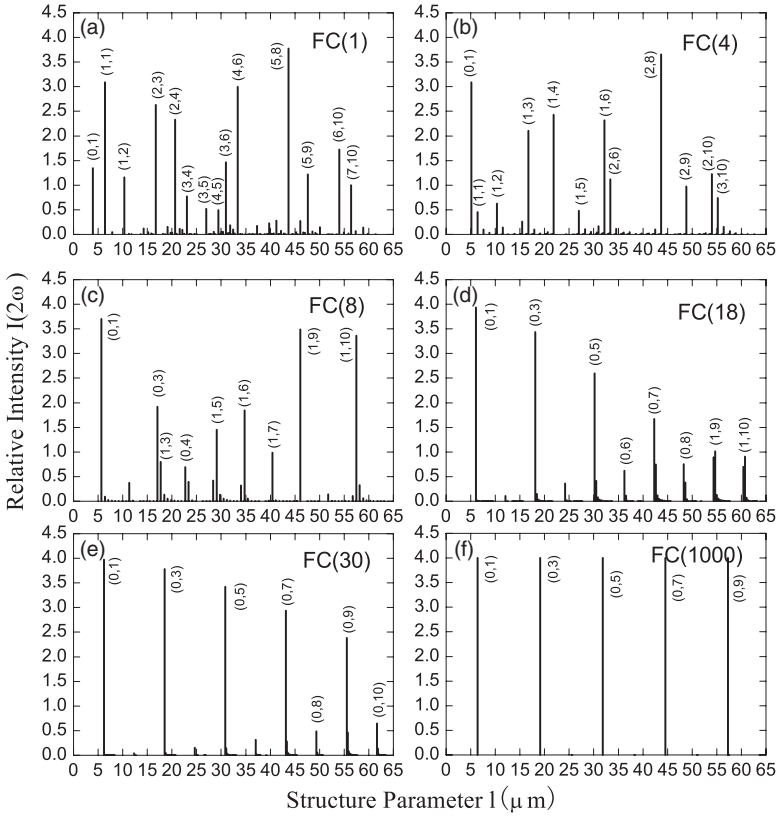

Figure 6. The SHG spectra for FC(n) ferroelectric superlattice systems in real space, where the corresponding parameters are the same as those in [10].

for GF(m, 1) superlattices there exists self-similarity for the structure parameter l of IPSHG under PQPM conditions, but this property would be broken under IQPM conditions.

In reciprocal space the wavelength of FB would vary, then generally the effect of the dispersion of refractive indices on SHG should be taken into account and the self-similarity would be destroyed, i.e. under IQPM and/or PQPM condition(s) there is no self-similarity for the count-down of wavelength λ.

5.2. The effect of the vacancies on the SHG spectra

From equation (24) one can see that for the output electric field of SHG E_2 there are two modulating factors $\sin \Delta kl/2$ and $\sin Y_{pq}$. If one of them is equal to zero some SHG peaks disappear, then one can obtain the following conditions for the effect of the vacancies on SHG spectra:

$$\begin{aligned} &\text{PQPM}: \quad \begin{cases} \text{(i)} \quad \{q, p\}_{\text{vacancy}} = \{0, 2n\} \\ \text{(ii)} \quad \{q, p\}_{\text{vacancy}} = \{n(m+1), n\} \end{cases} \\ &\text{IQPM}: \quad \begin{cases} \text{(i)} \quad \{q, p\}_{\text{vacancy}} = \{2n, 2n\} \\ \text{(ii)} \quad \{q, p\}_{\text{vacancy}} = \{n(m+1), n(2-m)\}, \qquad (m \leqslant 2), \end{cases} \end{aligned} \tag{46}$$

where n is a positive integer. Obviously, there are two different kinds of effects that the vacancies have on SHG spectra under PQPM and IQPM conditions, respectively, and all of the SHG spectral lines that have disappeared are weak lines.

Additionally, to the best of our knowledge there are very few reports of experimental measurements of the SHG effects in ferroelectric quasiperiodic superlattices. By means of $LiTaO_3$ and $Sr_{0.6}Ba_{0.4}Nb_2O_6$ materials, Ming *et al* [5, 32–34] designed and fabricated some optical superlattices following Fibonacci sequences and used these structures to measure the effects of quasi-phase-matching SHG and quasi-phase-matched third-harmonic generation. The most probable reasons for the lack of publications on non-Fibonaccian ferroelectric superlattices, we think, are the following: (1) compared with the Fibonacci model, the number of elements for GF(m, 1) sequences would increase quickly with increments in the generation number h and sequence parameter m. Consequently, the more blocks of ferroelectric domains there are, the more difficult it would be to fabricate the structures, and furthermore the more accumulated error would be caused; and (2) one usually calculates this kind of systems by use of the small-signal approximation method. If quasiperiodic systems are made up of too many domains, then the attenuation of signals should be taken into account. Therefore, experimenters would rather choose Fibonacci superlattices for simplicity.

6. Summary

First, we introduced the substitution method and the projection method for GF(m, 1). The characteristics of three important parameters θ, δ_m and τ_m were discussed.

Secondly, the formula of the output electric field of SHG E_2 was deduced under PQPM conditions. It was found that, when m changes from small to large, the structure, the relative intensity and the position of the SHG peaks all tend to be stable. If m is big enough, the two integers q and p indexing IPSHG make an interesting zero–odd set (see equation (29)).

Then, under IQPM conditions we analysed the tendency of SHG spectra and found that when m is large enough SHG spectra are made up of a group of intense peaks and another group of satellite weak lines, and the two integers q and p indexing these two kinds of SHG lines make a corresponding odd–odd set (see equation (39)) and a successive integer set (see equation (40)). In conclusion, GF(m, 1) are not perfect quasiperiodic sequences and the substitution method for generating GF(m, 1) is not completely in accord with the corresponding projection one. This means that the structures of GF(m, 1)s fitting PQPM conditions should be dependent on both irrationals. This is quite different from the case for the perfect quasiperiodic sequences.

Finally, we obtain the results for the self-similarity of intense peaks and the effect of vacancies on SHG and find that under PQPM conditions self-similarity of the intense peaks of SHG only exists in real space and it would be broken in reciprocal space. Two kinds of effects of vacancies on SHG have been found.

Acknowledgment

This work was supported by the National Natural Science Foundation of China, grant no 10004003.

References

[1] Shechtman D, Blech I, Gratias D and Cahn J W 1984 *Phys. Rev. Lett.* **53** 1951
[2] Merlin R, Bajema K, Clarke R, Juang F Y and Bhattacharya P K 1985 *Phys. Rev. Lett.* **55** 1768
[3] Tamura S and Wolfe J P 1987 *Phys. Rev.* B **36** 3491

[4] Zhu Y and Ming N 1990 *Phys. Rev.* B **42** 3676
[5] Zhu S, Zhu Y, Qin Y, Wang H, Ge C and Ming N 1997 *Phys. Rev. Lett.* **78** 2752
[6] Liu X, Wang Z, Wu J and Ming N 1998 *Chin. Phys. Lett.* **15** 426
[7] Liu X, Wang Z, Jiang X, Wu J and Ming N 1998 *J. Phys. D: Appl. Phys.* **31** 2502
[8] Chen Y, Zhu Y, Qin Y, Zhang C, Zhu S and Ming N 2000 *J. Phys.: Condens. Matter* **12** 529
[9] Chen Y, Zhang C, Zhu Y, Zhu S, Wang H and Ming N 2001 *Appl. Phys. Lett.* **78** 577
[10] Yang X and Liu Y 2000 *Eur. Phys. J.* B **15** 625
[11] Yang X and Liu Y 2000 *J. Phys.: Condens. Matter* **12** 1899
[12] Gumbs G and Ali M K 1988 *Phys. Rev. Lett.* **60** 1081
[13] Bombieri E and Taylor J E 1987 *J. Phys. Coll.* **48** C3 19
[14] Oh G Y and Lee M H 1993 *Phys. Rev.* B **48** 12465
[15] Dulea M, Severin M and Riklund R 1990 *Phys. Rev.* B **42** 3680
[16] Costa Filho R N and Albuquerque E L 1999 *Physica* A **274** 545
[17] Mauriz P W, Vasconcelos M S and Albuquerque E L 2003 *Physica* A **329** 101
[18] Tyc M H and Salejda W 2002 *Physica* A **303** 493
[19] Kohmoto M, Sutherland B and Iguchi K 1987 *Phys. Rev. Lett.* **58** 2436
[20] Klauzer-Kruszyna A, Salejda W and Tyc M H 2004 *Optik* **115** 257
[21] Klauzer-Kruszyna A, Salejda W and Tyc M H 2004 *Optik* **115** 267
[22] Li F and Yang X 2005 *Physica* B **368** 64
[23] Birch J, Severin M, Wahlström U, Yamamoto Y, Radnoczi G, Riklund R, Sundgren J E and Wallenberg L R 1990 *Phys. Rev.* B **41** 10398
[24] Zernike F and Midwinter J M 1973 *Applied Nonlinear Optics* (New York: Wiley) p 46
[25] Arecchi F T and Schulz-Du Bois E O 1972 *Laser Handbook* (Amsterdam: North-Holland) p 45
[26] Levine D and Steinhardt P J 1986 *Phys. Rev.* B **34** 596
[27] Bak P 1982 *Rep. Prog. Phys.* **45** 587
[28] Smith D S, Riccius H D and Edwin R P 1976 *Opt. Commun.* **17** 332
[29] Yao J, Li G, Xu J and Zhang G 1999 *Chin. J. Quantum Electron.* **16** 289
[30] Liu H, Zhu Y, Zhu S, Zhang C and Ming N 2001 *Appl. Phys. Lett.* **79** 728
[31] Fu X, Liu Y, Zhou P and Sritrakool W 1997 *Phys. Rev.* B **55** 2882
[32] Zhu S, Zhu Y and Ming N 1997 *Science* **278** 843
[33] Zhu Y, Xiao R, Fu J, Wang G and Ming N 1998 *Appl. Phys. Lett.* **73** 432
[34] Qin Y, Zhu Y, Zhu S and Ming N 1998 *J. Appl. Phys.* **84** 6911